Optimal Primary-User Mobility Aware Spectrum Sensing Design for Cognitive Radio Networks

Angela Sara Cacciapuoti, *Member, IEEE*, Ian F. Akyildiz, *Fellow, IEEE*, and Luigi Paura, *Member, IEEE*

***Abstract*—A key issue of the spectrum sensing functionality in Cognitive Radio (CR) networks is the ability of tuning the sensing time parameters, i.e., the sensing time and the transmission time, according to the Primary User (PU) network dynamics. In fact, these parameters influence both the spectrum sensing efficiency and the PU interference avoidance. This issue becomes even more challenging in presence of PU mobility. In this paper, an optimal spectrum sensing design for mobile PU scenarios is proposed with the aim to achieve the following important features: i) to determine the optimal mobility-aware transmission time, i.e., the transmission time value that jointly maximizes the spectrum sensing efficiency and satisfies the PU interference constraint; ii) to determine the optimal mobility-aware sensing time threshold, i.e., the maximum sensing time value assuring efficient spectrum sensing. First, closed-form expressions of both the optimal transmission time and the optimal sensing time threshold are analytically derived for a general PU mobility model. Then, the derived expressions are specialized for two widely adopted mobility models, i.e., the Random Walk mobility Model with reflection and the Random Way-Point mobility Model. Practical rules for the sensing parameter tuning are provided with reference to the considered mobility models. The analytical results are finally validated through simulations.**

***Index Terms*—Mobility, spectrum sensing, cognitive radio.**

I. Introduction

SPECTRUM Sensing is a key functionality in Cognitive Radio (CR) Networks [1]. Through spectrum sensing, unlicensed users (CR users) can recognize and dynamically exploit portions of the radio spectrum whenever they are vacated by licensed users, referred to as Primary Users (PUs).

The interference on the PU transmissions depends on the accuracy of the spectrum sensing, which, in static scenarios, is mainly affected by the wireless channel impairments, such as multipath fading and shadowing. Thus, recently, the research efforts have been devoted to improve the accuracy and the efficiency of sensing techniques [2]–[5].

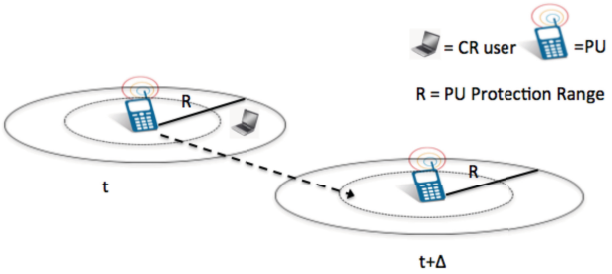

Fig. 1. The PU mobility changes the mutual distances between a PU and a CR user.

Despite these efforts, new challenges arise for the spectrum sensing design when the PUs are mobile. Mobility changes dynamically the mutual distances among the PUs and the CR users. As a consequence, the capability of the CR users to sense the PU transmissions varies in time. As an example, Fig. 1 shows a CR user that is inside the *protection range*[1] of a mobile PU at a certain time t. After the PU movement, say at time $t + \Delta$, the CR user is out of the PU protection range, thus becoming unable to sense the possible PU transmissions.

In [7], we study the aforementioned effects of the PU mobility on the sensing capability by analytically deriving two performance metrics: i) the *detection capability*, i.e., the probability of a CR user being inside the protection range of a PU, which measures the mobility impact on the CR detection probability; ii) the *mobility-enabled sensing capacity*, i.e., the expected transmission capacity achievable by a CR user in presence of PU mobility. The results show that the PU mobility can increase the sensing capacity achievable by the CR users.

Although some interesting results are obtained in [7], some of the important issues are still open. For example, the key issue of *how to revise the current design of the spectrum sensing functionality in presence of PU mobility* is still an open problem. The spectrum sensing functionality must be able to tune its time parameters, i.e., the *sensing time* and the *transmission time*, according to the mobile PU dynamics. The sensing time and the transmission time influence both the sensing efficiency and the PU interference avoidance [2]. Hence, the proper selection of the sensing time parameters is crucial for the performance of a CR network.

[1]To avoid harmful interference against the PUs, the CR users should detect active PUs within a range, referred to as *protection range*, determined by the PU transmission range and by the CR interference range[6].

Manuscript received April 15, 2012, revised August 31, 2012.

A. S. Cacciapuoti was with the Broadband Wireless Networking Laboratory, School of Electrical and Computer Engineering, Georgia Institute of Technology, USA. She is now with the Department of Electric Engineering and Information Technology, University of Naples Federico II, Italy (e-mail: angelasara.cacciapuoti@unina.it).

I. F. Akyildiz is with the Broadband Wireless Networking Laboratory, School of Electrical and Computer Engineering, Georgia Institute of Technology, Atlanta, GA 30332, USA (e-mail: ian@ece.gatech.edu).

L. Paura is with the Department of Electric Engineering and Information Technology, University of Naples Federico II, Naples, Italy (e-mail: paura@unina.it).

This work was supported by the Italian National Program under Grants PON01-00744, "DRIVE-IN2: DRIVEr monitoring: Technologies, methodologies, and IN-vehicle INnovative systems for a safe and ecocompatible driving" and PON01-01936, "HABITAT: HarBour traffIc opTimizAtion sysTem," by the University of Naples Federico II under Award "Programma di scambi internazionali tra l'Universitá degli Studi di Napoli Federico II ed Universitá ○ Istituti di ricerca stranieri," and by the U.S. National Science Foundation under Award ECCS-0900930.

Digital Object Identifier 10.1109/JSAC.2013.131102

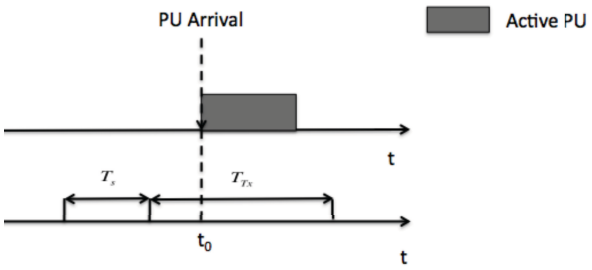

Fig. 2. An active mobile PU arrives during the CR Transmission Time.

To this aim, in this paper, we derive the *optimal values* for both the transmission time and the sensing time in presence of PU mobility.

More specifically, regarding the transmission time, we derive an optimal closed-form expression, i.e., the transmission time value that jointly maximizes the spectrum sensing efficiency and satisfies the PU interference constraint.

Regarding the sensing time, we prove that in mobile scenarios the sensing accuracy exhibits a threshold behavior as a function of the sensing time. That means the sensing accuracy can decrease for sensing times longer than the threshold value[2]. This is an important result compared to static scenarios where it is well known that longer sensing times lead to higher sensing accuracy [2], [3]. We also provide an optimal closed-form expression for the sensing time threshold.

All theoretical results are first derived by adopting a general PU mobility model. Then, they are specialized for two widely adopted mobility models [8], i.e., the Random Walk mobility Model with reflection (RWM) and the Random Way-Point mobility Model (RWPM). Moreover, the obtained results are exploited to single out practical rules for the sensing parameter tuning.

The rest of the paper is organized as follows. In Section II, we present the problem statement and discuss the relevant related work. In Section III, we describe the system model. In Section IV, we present intermediate results that will be used in Section V to derive the optimal sensing time parameters. We validate the analytical results by simulation in Section VI. In Section VII, we discuss the derived results and we provide insights for future research. In Section VIII, we conclude the paper, and, finally, some proofs are demonstrated in the appendices.

II. Problem Statement

Let us consider a typical sensing scenario in which a CR user monitors a spectrum band licensed to a mobile PU. The CR user alternately senses the spectrum during the *sensing time* $T_{\rm s}$ and transmits data during the *transmission time* $T_{\rm Tx}$.

A. Challenges

In static scenarios, the sensing and the transmission times depend mainly on three factors: i) the adopted spectrum sensing technique; ii) the required interference constraint on the PU transmissions; iii) the PU traffic dynamics. In mobile scenarios, the sensing and the transmission times depend also on the PU mobility.

- *Transmission Time Challenges*:
  Even if the spectrum sensing process is ideal, i.e., it is not affected by errors, in mobile scenarios the probability of a CR user to interfere the PU transmissions can be different from zero. As an example, let us consider Fig. 2. At the end of the sensing time $T_{\rm s}$, the CR user correctly decides to use the monitored spectrum band, since it does not detect any PU transmission during such a sensing time. However, at time $t_0 \in T_{\rm Tx}$ a mobile PU enters in the CR interference region (see Def. 3, Section III). As a consequence, if the PU is active, the CR user interferes the PU, despite the perfect sensing decision.
- *Sensing Time Challenges*:
  In mobile scenarios, the classical statement that holds in static scenarios, i.e., longer sensing time leads to higher detection accuracy, does not hold necessarily. As a simple example, let us consider a CR user characterized by a probability of being inside the PU protection range lower than the maximum interference probability (see Def. 9, Section III) tolerated by the PU. In such a case, it is useless to perform spectrum sensing, i.e., the sensing time should be set equal to zero. In fact, the probability that the CR user interferes the PU transmissions is lower than the PU interference constraint. Indeed, as mentioned in Section I, we will prove through the paper that, for sensing times longer than a threshold value, the sensing accuracy can decrease. As a consequence, determining the threshold value of the sensing time is a key factor for an effective spectrum sensing in mobile PU scenarios.

B. Optimal PU-Mobility Aware Spectrum Sensing Design

In this paper, we propose a novel spectrum sensing design for mobile PU scenarios with the objective to overcome the aforementioned issues. More in detail:

- we derive a closed-form expression of the optimal mobility-aware transmission time for a general PU mobility model;
- we provide practical rules, based on a lower bound of the optimal transmission time, for setting the transmission time when the PUs move according to the RWM and RWPM;
- we derive a closed-form expression of the optimal mobility-aware sensing time threshold for a general PU mobility model;
- we provide practical rules, based on the optimal sensing time threshold, for setting the sensing time when the PUs move according to the RWM and RWPM.

Moreover, stemming from the obtained results, we analytically evaluate the sensing efficiency, and we prove that the sensing efficiency can increase in presence of PU mobility.

C. Related Work

In general, both the CR users and the PUs are assumed to be static in the literature. As a consequence, to the best of

[2]Clearly, the sensing accuracy strictly depends on the adopted sensing technique. Nevertheless, in the following we prove that, regardless of the adopted sensing technique, the sensing accuracy exhibits the aforementioned threshold behavior as a consequence of the mobile PU dynamics.

our knowledge, the analysis of the effects of the user mobility on spectrum sensing is still an open research problem in the literature.

In [9], the authors take into account the CR user mobility by modeling the CR channel availability as a two-state continuous-time Markov chain. Stemming from this model, the authors propose the use of a guard distance, i.e., an additional separation between PUs and CR users, to prevent excessive interference on the PU transmissions. Then, they jointly optimize the guard distance and the sensing time to maximize the reuse of spectrum opportunities. In [10], the authors develop a correlation-aware user selection to address the dynamic changes in the spatial correlation experienced by mobile CR users, with the objective to increase the performance of cooperative spectrum sensing. The proposed user selection is location-unaware, fully distributed and adaptive. In [11], the authors model the PU network as a random geometric network to describe the random locations experienced by small-scale mobile PUs. Stemming from this model, the authors propose a location-aware cooperative sensing algorithm that linearly combines the sensing results from multiple CR users.

Unlike all the aforementioned works, in this paper, we address the issue of the optimal selection of the sensing time and the transmission time in presence of PU mobility.

III. System Model and Preliminaries

In this section, we first describe the system model. Then, we collect several definitions that will be used through the paper.

A. Network Models

PU Network Model: The PUs move according to a general mobility model in a network region $\boldsymbol{A}$, assumed, without loss of generality, either as a line or as a square. $f_{\boldsymbol{X}_{\rm PU}}(\boldsymbol{x}_{\rm PU})$ denotes the probability density function (pdf) of the PU steady-state spatial distribution, and R is the PU protection radius. The PU traffic is modeled as a two state birth-death process [2], [7], with death rate α and birth rate β. In the "*on*" state the PU is active with probability $P_{\rm on} = \beta/(\alpha+\beta)$, whereas in the "*off*" state it is inactive with probability $P_{\rm off} = \alpha/(\alpha+\beta)$.

CR User Network Model: The CR users are assumed static and uniformly distributed in the network region $\boldsymbol{A}$. $f_{\boldsymbol{X}_{\rm CR}}(\boldsymbol{x}_{\rm CR})$ denotes the pdf of the CR user spatial distribution.

B. Definitions and Assumptions

Definition 1. Event $\mathcal{I}$: "The CR user is inside the PU protection range."

Definition 2. Event $\mathcal{O}$: "The CR user is out of the PU protection range."

Definition 3. An arbitrary CR user is inside the protection range R of a mobile PU if the PU is placed within a disk $\boldsymbol{C}(\boldsymbol{x}_{\rm CR})$ of radius R around the CR user location $\boldsymbol{x}_{\rm CR}$, i.e., if the Euclidean distance between the CR user and the PU is not greater than R. In the following, we refer to $\boldsymbol{C}(\boldsymbol{x}_{\rm CR})$ as *CR interference region*.

Assumption 1. The PUs move according to a memoryless mobility pattern constituted by a sequence of movement periods. During each movement period, a PU does not change its direction and its velocity.

Remark 1. Assumption 1 is not restrictive since it is verified by a large number of very popular mobility models, such as the random walk and its derivatives, the random waypoint, the random direction mobility model and many others [8].

Definition 4. The random variable (r.v.) L, denoting the Euclidean distance covered by a PU during a movement period, is referred to as *movement length*. The r.v. D, denoting the time spent by a PU to complete a movement, is referred to as *movement duration*. D includes also the possible pause time spent by a PU in the same location at the end of a movement.

Definition 5. Let us consider a PU moving according to a general mobility model and starting from its steady-state spatial distribution. The out time Θ is the time interval the PU spends out of the interference region of an arbitrary CR user:

$$\begin{aligned}\Theta \stackrel{\triangle}{=} \inf_{t>t_1}\{t-t_1 : ||\boldsymbol{X}_{\rm PU}(t)-\boldsymbol{X}_{\rm CR}|| \le R \wedge \\ \left|\left|\boldsymbol{X}_{\rm PU}(t_1^-)-\boldsymbol{X}_{\rm CR}\right|\right| \le R \wedge \left|\left|\boldsymbol{X}_{\rm PU}(t_1^+)-\boldsymbol{X}_{\rm CR}\right|\right| > R\}\end{aligned} \tag{1}$$

where $\wedge$ denotes the logical operator *and*.

Definition 6. Let us consider a PU moving according to a general mobility model and starting from its steady-state spatial distribution. The sojourn time $\mathcal{S}$ is the time interval a PU spends inside the interference region of an arbitrary CR user:

$$\begin{aligned}\mathcal{S} \stackrel{\triangle}{=} \sup_{t>t_0}\{t-t_0 : ||\boldsymbol{X}_{\rm PU}(t)-\boldsymbol{X}_{\rm CR}|| \le R\} \wedge \\ \left|\left|\boldsymbol{X}_{\rm PU}(t_0^-)-\boldsymbol{X}_{\rm CR}\right|\right| > R \wedge \left|\left|\boldsymbol{X}_{\rm PU}(t_0^+)-\boldsymbol{X}_{\rm CR}\right|\right| \le R\}\end{aligned} \tag{2}$$

where $\wedge$ denotes the logical operator *and*.

Definition 7. Let us consider a PU moving according to a general mobility model and starting from its steady-state spatial distribution. The inter-arrival time $\mathcal{T}$ is the time interval between two consecutive arrivals of the PU in the interference region of an arbitrary CR user. By accounting for Def. 5 and Def. 6, it is clear that:

$$\mathcal{T} = \mathcal{S} + \Theta \tag{3}$$

Definition 8. Let us consider a mobile PU that moves according to a general mobility model satisfying Assumption 1 and starting from its steady-state spatial distribution. The r.v. $\mathcal{M}$ denotes the number of movement periods a PU takes to enter in a CR interference region.

Definition 9. The *maximum interference probability* $P_{\rm int}$ is the maximum value of the interference probability that an arbitrary CR user can cause on the PU transmissions[3].

[3] $P_{\rm int}$ accounts for two factors: i) the level of interference tolerated by the PU network; ii) the spectrum sensing accuracy.

IV. Primary-User Inter-Arrival Process

Here, we first characterize the PU inter-arrival time for a general mobility model by deriving closed-form expressions for both its average value (*Theorem* 1) and its Cumulative Distribution Function (CDF) (*Theorem* 2). Then, we specialize the derived results for the RWM and for the RWPM. These results will be used in Section V to determine the optimal sensing time parameters.

A. General Mobility Model

The proofs of Theorem 1 and Theorem 2 require two intermediate results, i.e., Proposition 1 and Proposition 2.

Proposition 1. *Let us consider a CR user at a certain location $\boldsymbol{x}_{CR} \in \boldsymbol{A}$. The distribution of the r.v. $\mathcal{M}$ conditioned to $\boldsymbol{x}_{CR}$ is geometric with parameter $P_g(\boldsymbol{x}_{CR})$, i.e.:*

$$P(\mathcal{M} > k|\boldsymbol{x}_{CR}) = (1 - P_g(\boldsymbol{x}_{CR}))^k = \\ = \left(1 - \int_{\mathcal{L}} \int_{\boldsymbol{C}(\boldsymbol{x}_{CR},l)} f_{\boldsymbol{X}_{PU}}(\boldsymbol{x}_{PU}) d\boldsymbol{x}_{PU}\, f_L(l)\, dl\right)^k \quad (4)$$

where $\boldsymbol{C}(\boldsymbol{x}_{CR}, l) \in \boldsymbol{A}$ is a region around $\boldsymbol{x}_{CR}$ depending on the r.v. L, whose pdf is $f_L(l)$.

Proof: See Appendix A. ∎

Proposition 2. *The average out time $\overline{\Theta} \triangleq E[\Theta]$ of a PU roaming within a network region $\boldsymbol{A}$ according to a general mobility model is given by:*

$$\overline{\Theta} = \overline{D} \int_{\boldsymbol{A}} \frac{f_{\boldsymbol{X}_{CR}}(\boldsymbol{x}_{CR}) d\boldsymbol{x}_{CR}}{\int_{\mathcal{L}} \int_{\boldsymbol{C}(\boldsymbol{x}_{CR},l)} f_{\boldsymbol{X}_{PU}}(\boldsymbol{x}_{PU}) d\boldsymbol{x}_{PU}\, f_L(l) dl} \quad (5)$$

where[4] *$\overline{D} \triangleq E[D]$ is the expected value of the r.v. D.*

Proof: See Appendix B. ∎

Theorem 1. *The average inter-arrival time $\overline{\mathcal{T}} \triangleq E[\mathcal{T}]$ of a PU roaming within a network region $\boldsymbol{A}$ according to a general mobility model is given by:*

$$\overline{\mathcal{T}} = \frac{\overline{\Theta}}{1 - P(\mathcal{I})} = \frac{\overline{D} \int_{\boldsymbol{A}} \frac{f_{\boldsymbol{X}_{CR}}(\boldsymbol{x}_{CR}) d\boldsymbol{x}_{CR}}{\int_{\mathcal{L}} \int_{\boldsymbol{C}(\boldsymbol{x}_{CR},l)} f_{\boldsymbol{X}_{PU}}(\boldsymbol{x}_{PU}) d\boldsymbol{x}_{PU}\, f_L(l) dl}}{1 - P(\mathcal{I})} \quad (6)$$

where $P(\mathcal{I})$ is the probability of the event $\mathcal{I}$.

Proof: Stemming from (3), we have:

$$\overline{\mathcal{T}} \triangleq E[\mathcal{T}] = E[\mathcal{S}] + E[\Theta] \triangleq \overline{\mathcal{S}} + \overline{\Theta} \quad (7)$$

Since $P(\mathcal{I})$ represents the percentage of time the CR user is located within the PU protection range, by applying the Little's Theorem [12], we obtain:

$$\overline{\mathcal{S}} = P(\mathcal{I})\, \overline{\mathcal{T}} \quad (8)$$

By substituting (8) in (7) and by accounting for (5), the proof follows. ∎

[4]In (5), $\int_{\boldsymbol{A}}(\cdot)\, d\boldsymbol{x}$ and $\int_{\boldsymbol{C}(\boldsymbol{x}_{\rm CR},l)}(\cdot)\, d\boldsymbol{x}$ are double integrals if $\boldsymbol{A}$ denotes a bi-dimensional network region, otherwise they are single integrals.

Both (5) and (6) are general since they hold for every mobility model satisfying Assumption 1.

Remark 2. From (6), it results that $\overline{\mathcal{T}}$ depends on three factors: i) the PU mobility model, through the PU steady-state spatial distribution $f_{\boldsymbol{X}_{\rm PU}}(\cdot)$, $\overline{D}$, and $f_L(l)$; ii) the CR spatial distribution $f_{\boldsymbol{X}_{\rm CR}}(\cdot)$; iii) the probability $P(\mathcal{I})$ of an arbitrary CR user being inside the PU protection range.

Theorem 2. *The CDF $\mathcal{F}_{\mathcal{T}}(t) \triangleq P(\mathcal{T} \leq t)$ of the inter-arrival time $\mathcal{T}$ of a PU roaming within a network region $\boldsymbol{A}$ according to a general mobility model is bounded as follows:*

$$\mathcal{F}_{\mathcal{T}}(t) \triangleq P(\mathcal{T} \leq t) \leq 1 - \int_{\boldsymbol{A}} e^{-\frac{t}{\overline{D}} P_g(\boldsymbol{x}_{CR})} f_{\boldsymbol{X}_{CR}}(\boldsymbol{x}_{CR}) d\boldsymbol{x}_{CR} \quad (9)$$

where $P_g(\boldsymbol{x}_{CR})$ is given in Proposition 1.

Proof: See Appendix C. ∎

B. Random Walk Mobility Model

Here, we specialize Theorem 1 and Theorem 2 when the PU is roaming according to the RWM within both a one-dimensional and a bi-dimensional network region $\boldsymbol{A}$. Under the RWM, a PU randomly chooses both a direction and a velocity according to a uniform distribution in the intervals $[0, 2\pi]$ and $[v_{\min}, v_{\max}]$ m/s, respectively. Each movement occurs in a constant time. At the end of each movement, a new direction and speed are calculated according to the same rule. When the edge of the network region $\boldsymbol{A}$ is reached, the PU is bounced back to the region. This model produces a uniform steady-state spatial distribution regardless of the average PU speed [13].

Theorem 1 for RWM: The average inter-arrival time $\overline{\mathcal{T}}_{\rm RWM}$ of a PU roaming within a network region $\boldsymbol{A}$ according to the RWM is given by:

$$\overline{\mathcal{T}}_{\rm RWM} = \frac{\overline{\Theta}_{\rm RWM}}{1 - P_{\rm RWM}(\mathcal{I})} = \\ = \begin{cases} \frac{a}{\overline{v}_{\rm RWM}(1 - P_{\text{1D-RWM}}(\mathcal{I}))}, & A = [0, a] \\ \\ \frac{a^2}{2\, R\, \overline{v}_{\rm RWM}(1 - P_{\text{2D-RWM}}(\mathcal{I}))}, & \boldsymbol{A} = [0, a] \times [0, a] \end{cases} \quad (10)$$

where $P_{\text{1D-RWM}}(\mathcal{I}) = 2\left(\frac{R}{a}\right) - \left(\frac{R}{a}\right)^2$, $P_{\text{2D-RWM}}(\mathcal{I}) = \pi\left(\frac{R}{a}\right)^2 - \frac{8}{3}\left(\frac{R}{a}\right)^3 + \frac{1}{2}\left(\frac{R}{a}\right)^4$ [7], $\overline{v}_{\rm RWM} = \frac{v_{\min} + v_{\max}}{2}$ denotes the average PU velocity, a is the size of the one-dimensional network region $A = [0, a]$ and a^2 is the size of the bi-dimensional network region $\boldsymbol{A} = [0, a] \times [0, a]$.

Proof: See Appendix D. ∎

Remark 3. The derived $\overline{\mathcal{T}}_{\rm RWM}$ depends on three factors: i) the average PU velocity $\overline{v}_{\rm RWM}$, ii) the normalized protection radius R/a; iii) the size of the network region $\boldsymbol{A}$.

Theorem 2 for RWM: The CDF $\mathcal{F}_{\mathcal{T}_{\rm RWM}}(t)$ of the inter-arrival time $\mathcal{T}_{\rm RWM}$ of a PU roaming within a network region $\boldsymbol{A}$ according to the RWM is bounded by an exponential distribution $\mathcal{E}_{\Omega_{\rm RWM}}(t)$ of parameter $\Omega_{\rm RWM}$:

$$\mathcal{F}_{\mathcal{T}_{\rm RWM}}(t) \triangleq P(\mathcal{T}_{\rm RWM} \leq t) \leq 1 - e^{-\Omega_{\rm RWM}\, t} \triangleq \mathcal{E}_{\Omega_{\rm RWM}}(t) \quad (11)$$

where

$$\Omega_{\text{RWM}} \triangleq \frac{1}{\overline{\Theta}_{\text{RWM}}} = \begin{cases} \frac{\overline{v}_{\text{RWM}}}{a}, & A = [0,a] \\ \frac{2\,R\,\overline{v}_{\text{RWM}}}{a^2}, & \boldsymbol{A} = [0,a]\times[0,a] \end{cases} \tag{12}$$

Proof: See Appendix D. ∎

C. Random WayPoint Mobility Model

Here, we specialize *Theorem* 1 and *Theorem* 2 when the PU is roaming according to the RWPM within both a one-dimensional and a bi-dimensional network region $\boldsymbol{A}$. Under the RWPM, a PU randomly chooses a destination inside $\boldsymbol{A}$ according to a uniform distribution, and it moves towards this destination with a velocity chosen uniformly at random in the interval $[v_{\min}, v_{\max}]$ m/s. When the PU reaches its destination, it starts moving again according to the same rule[5]. This model produces a non-uniform steady-state spatial distribution [14].

Theorem 1 for RWPM: The average inter-arrival time $\overline{\mathcal{T}}_{\text{RWPM}}$ of a PU roaming within a network region $\boldsymbol{A}$ according to the RWPM is given by:

$$\overline{\mathcal{T}}_{\text{RWPM}} = \frac{\overline{\Theta}_{\text{RWPM}}}{1 - P_{\text{RWPM}}(\mathcal{I})} = \tag{13}$$
$$= \begin{cases} \frac{2\,a}{3\,\overline{v}_{\text{RWPM}}}\,\frac{\tanh^{-1}\left(1-\frac{\overline{L}}{a}\right)}{(1-P_{\text{1D-RWPM}}(\mathcal{I}))}, & A = [0,a] \\ \frac{2\,a^2}{9\,R\,\overline{v}_{\text{RWPM}}}\,\frac{\tanh^{-1}\left(1-\frac{\overline{L}}{a}\right)\tanh^{-1}\left(1-\frac{2R}{a}\right)}{(1-P_{\text{2D-RWPM}}(\mathcal{I}))}, & \boldsymbol{A} = [0,a]\times[0,a] \end{cases}$$

where $P_{\text{1D-RWPM}}(\mathcal{I}) = 2\left(\frac{R}{a}\right) - 2\left(\frac{R}{a}\right)^3 + \left(\frac{R}{a}\right)^4$, $P_{\text{2D-RWPM}}(\mathcal{I}) = \pi\left(\frac{R}{a}\right)^2 - \frac{3\pi}{2}\left(\frac{R}{a}\right)^4 + \frac{32}{15}\left(\frac{R}{a}\right)^5 + \frac{3\pi}{8}\left(\frac{R}{a}\right)^6 - \frac{32}{35}\left(\frac{R}{a}\right)^7 + \frac{1}{6}\left(\frac{R}{a}\right)^8$ [7], $\overline{v}_{\text{RWPM}} \triangleq \frac{v_{\max}-v_{\min}}{\log(v_{\max}/v_{\min})}$ and $\tanh^{-1}(\cdot)$ denotes the inverse hyperbolic tangent function.

Proof: See Appendix E. ∎

Remark 4. The derived $\overline{\mathcal{T}}_{\text{RWPM}}$ depends on four factors: i) the average PU velocity $\overline{v}_{\text{RWPM}}$ (footnote 9, Appendix E); ii) the normalized protection radius R/a; iii) the size of the network region $\boldsymbol{A}$; iv) the average movement length $\overline{L}$, equal to $\overline{L} = a/3$ for one-dimensional network regions and equal to $\overline{L} \simeq 0.5214\,a$ for squared bi-dimensional network regions [14].

Theorem 2 for RWPM: The CDF $\mathcal{F}_{\mathcal{T}_{\text{RWPM}}}(t)$ of the inter-arrival time $\mathcal{T}_{\text{RWPM}}$ of a PU roaming within a network region $\boldsymbol{A}$ according to the RWPM is bounded by an exponential distribution $\mathcal{E}_{\Psi_{\text{RWPM}}}(t)$ of parameter Ψ_{RWPM}:

$$\mathcal{F}_{\mathcal{T}_{\text{RWPM}}}(t) \triangleq P(\mathcal{T}_{\text{RWPM}} \leq t) \leq \tag{14}$$
$$\leq 1 - {}_1F_1\left(\frac{1}{2};\frac{3}{2};\Psi_{\text{RWPM}}t\right) e^{-\Psi_{\text{RWPM}}t} \leq 1 - e^{-\Psi_{\text{RWPM}}\,t}$$

where, $1 - {}_1F_1\left(\frac{1}{2};\frac{3}{2};\Psi_{\text{RWPM}}t\right) e^{-\Psi_{\text{RWPM}}t} =$

$$\begin{cases} 1 - e^{-\Psi_{\text{RWPM}}t}, & \Psi_{\text{RWPM}}\,t \to 0 \\ 1, & \Psi_{\text{RWPM}}\,t \to \infty, \\ 1 - {}_1F_1\left(\frac{1}{2};\frac{3}{2};\Psi_{\text{RWPM}}t\right) e^{-\Psi_{\text{RWPM}}\,t}, & \text{otherwise} \end{cases}$$

with ${}_1F_1\,(d;f;u)$ denoting the Kummer confluent hypergeometric function [15], and

$$\Psi_{\text{RWPM}} \triangleq \frac{\varphi\left(\overline{L},R,a\right)}{\overline{\Theta}_{\text{RWPM}}} = \tag{15}$$
$$\begin{cases} \frac{\tanh^{-1}\left(1-\frac{\overline{L}}{a}\right)}{\overline{\Theta}_{\text{1D-RWPM}}} = \frac{3\,\overline{v}_{\text{RWPM}}}{2\,a}, & A = [0,a] \\ \frac{\tanh^{-1}\left(1-\frac{\overline{L}}{a}\right)\tanh^{-1}\left(1-\frac{2R}{a}\right)}{\overline{\Theta}_{\text{2D-RWPM}}} = \frac{9R\,\overline{v}_{\text{RWPM}}}{2\,a^2}, & \boldsymbol{A} = [0,a]\times[0,a] \end{cases}$$

Proof: See Appendix E. ∎

Remark 5. When $\Psi_{\text{RWPM}}\,t \to 0$, $1 - {}_1F_1\left(\frac{1}{2};\frac{3}{2};\Psi_{\text{RWPM}}t\right) e^{-\Psi_{\text{RWPM}}t} \to 1 - e^{-\Psi_{\text{RWPM}}t}$. As a consequence, when $\Psi_{\text{RWPM}}\,t \to 0$, $\mathcal{F}_{\mathcal{T}_{\text{RWPM}}}(t)$ is directly bounded by $1 - e^{-\Psi_{\text{RWPM}}\,t}$.

V. Primary-User Mobility Aware Sensing Design

Here, we first derive the closed-form expressions for both the optimal transmission time and the optimal sensing time threshold. Then, we provide practical rules for setting both the transmission and the sensing times when the PU moves according to the RWM and RWPM. Finally, we analytically evaluate the mobility-aware sensing efficiency.

A. Optimal Mobility-Aware Transmission Time

Definition 10. The optimal mobility-aware transmission time is defined as the transmission time that $i)$ allows a CR user to respect the PU interference constraint in mobile PU environments, $ii)$ maximizes the sensing efficiency for a given value of the sensing time.

Proposition 3. *Let us consider a PU roaming within a network region $\boldsymbol{A}$ according to a general mobility model. The optimal mobility-aware transmission time T_{Tx}^{opt} is equal to:*

$$T_{Tx}^{opt} = \mathcal{F}_{\mathcal{T}}^{-1}\left(\frac{P_{int}}{P_{on}}\right) \tag{16}$$

where $\mathcal{F}_{\mathcal{T}}(t)$ is the CDF of the PU inter-arrival time $\mathcal{T}$, P_{on} is the PU on-state probability, and P_{int} is the maximum interference probability.

Proof: During two PU arrival events in a CR interference region, a CR user can interferes an active PU during the transmission time T_{Tx}. As a consequence, T_{Tx} cannot exceed the maximum interference time an *active* PU can tolerate between two arrival events, i.e.:

$$\mathcal{F}_{\mathcal{T}}(T_{\text{Tx}})P_{\text{on}} = P\left(\mathcal{T} \leq T_{\text{Tx}}\right)P_{\text{on}} \leq P_{\text{int}} \Leftrightarrow T_{\text{Tx}} \leq \mathcal{F}_{\mathcal{T}}^{-1}\left(\frac{P_{\text{int}}}{P_{\text{on}}}\right) \tag{17}$$

According to Def. 10, the proof follows by considering the maximum T_{Tx} satisfying (17). ∎

[5]Without loss of generality, we consider the classical version of the RWPM without pause times. The developed analysis is immediately generalizable to the RWPM with pause times, by including in $\overline{D}$ also the average pause time, and by using the expression of $P(\mathcal{I})$ derived in [7] for non-zero pause times.

B. Optimal Mobility-Aware Transmission Time for RWM and RWMP

Here, we exploit Prop. 3 for deriving a lower bound of $T_{\text{Tx}}^{\text{opt}}$ for both the RWM and the RWPM.

Theorem 3. *When a PU is roaming within a network region $\boldsymbol{A}$ according to the RWM, the optimal transmission time $T_{Tx\text{-}RWM}^{opt}$ satisfies the following inequality:*

$$T_{Tx\text{-}RWM}^{opt} \geq \overline{\Theta}_{RWM} \log\left(\frac{P_{on}}{P_{on}-P_{int}}\right), \quad P_{on} \geq P_{int} \tag{18}$$

where the average PU out time $\overline{\Theta}_{RWM}$ is given in (12) *for both one-dimensional and bi-dimensional network region $\boldsymbol{A}$.*

Proof: To assure a certain P_{int}, we need to satisfy (16), i.e., $T_{\text{Tx-RWM}}^{\text{opt}} = \mathcal{F}_{\text{PU-RWM}}^{-1}\left(\frac{P_{\text{int}}}{P_{\text{on}}}\right)$. Let us denote with T_x the time value satisfying the same constraint P_{int} for the exponential distribution $\mathcal{E}_{\Omega_{\text{RWM}}}(t)$ (11), i.e., $T_x = \mathcal{E}_{\Omega_{\text{RWM}}}^{-1}\left(\frac{P_{\text{int}}}{P_{\text{on}}}\right)$. By exploiting the bound derived in Theorem 2 for the RWM, the proof follows:

$$\begin{aligned} T_{\text{Tx-RWM}}^{\text{opt}} &= \mathcal{F}_{\text{PU-RWM}}^{-1}\left(\frac{P_{\text{int}}}{P_{\text{on}}}\right) \geq T_x = \mathcal{E}_{\Omega_{\text{RWM}}}^{-1}\left(\frac{P_{\text{int}}}{P_{\text{on}}}\right) = \\ &= \overline{\Theta}_{\text{RWM}} \log\left(\frac{P_{\text{on}}}{P_{\text{on}}-P_{\text{int}}}\right) \end{aligned} \tag{19}$$

■

Theorem 4. *When a PU is roaming within a network region $\boldsymbol{A}$ according to the RWPM, the optimal transmission time $T_{Tx\text{-}RWPM}^{opt}$ satisfies the following inequality:*

$$T_{Tx\text{-}RWPM}^{opt} \geq \frac{\overline{\Theta}_{RWPM}}{\varphi\left(\overline{L},R,a\right)} \log\left(\frac{P_{on}}{P_{on}-P_{int}}\right), \quad P_{on} \geq P_{int} \tag{20}$$

where $\frac{\overline{\Theta}_{RWPM}}{\varphi\left(\overline{L},R,a\right)}$ is the normalized average PU out time given in (15) *for both one-dimensional and bi-dimensional network region $\boldsymbol{A}$.*

Proof: As for the RWM, by using the result of Theorem 2 for RWPM, we have:

$$\begin{aligned} T_{\text{Tx-RWPM}}^{\text{opt}} &= \mathcal{F}_{\text{PU-RWPM}}^{-1}\left(\frac{P_{\text{int}}}{P_{\text{on}}}\right) \geq \mathcal{E}_{\Psi_{\text{RWPM}}}^{-1}\left(\frac{P_{\text{int}}}{P_{\text{on}}}\right) = \\ &= \frac{\overline{\Theta}_{\text{RWPM}}}{\varphi\left(\overline{L},R,a\right)} \log\left(\frac{P_{\text{on}}}{P_{\text{on}}-P_{\text{int}}}\right) \end{aligned} \tag{21}$$

■

Remark 6. For both the RWM and RWPM: i) if $P_{\text{on}} = P_{\text{int}}$, $T_{\text{Tx}}^{\text{opt}} \to \infty$, i.e., if the interference constraint is equal to P_{on}, a CR user can transmit for an infinite time; ii) $T_{\text{Tx}}^{\text{opt}}$ increases as $\overline{\Theta}$ increases, since the PU spends more time out of the CR interference region.

Insight 1 (Mobility-Aware Transmission Time)**.** (18) and (20) provide practical rules for setting the transmission time T_{Tx}. In fact: i) transmission times shorter than the derived bounds cause spectrum sensing inefficiency; ii) transmission times longer than the derived bounds can violate the PU interference constraint. Hence, T_{Tx} can be set as follows:

$$\begin{aligned} T_{\text{Tx-RWM}} &= \overline{\Theta}_{\text{RWM}} \log\left(\frac{P_{\text{on}}}{P_{\text{on}}-P_{\text{int}}}\right) \\ T_{\text{Tx-RWPM}} &= \frac{\overline{\Theta}_{\text{RWPM}}}{\varphi\left(\overline{L},R,a\right)} \log\left(\frac{P_{\text{on}}}{P_{\text{on}}-P_{\text{int}}}\right) \end{aligned} \tag{22}$$

C. Optimal Mobility-Aware Sensing Time Threshold

Definition 11. The optimal sensing time threshold is the value of the sensing time assuring that the sensing accuracy does not increase by observing the spectrum band for times longer than the optimal sensing time threshold, regardless of the adopted spectrum sensing technique.

Proposition 4. *Let us consider a PU roaming within a network region $\boldsymbol{A}$ according to a general mobility model. The mobility-aware sensing time T_s must be set as follows:*

$$T_s \leq \overline{\mathcal{S}} \tag{23}$$

where $\overline{\mathcal{S}}$ is the average sojourn time (8) *of a mobile PU inside the CR interference region.*

Proof: Y and γ denote the decision variable and threshold of a generic sensing technique, respectively. $\mathcal{H}_0$ and $\mathcal{H}_1$ denote the hypotheses of "no PU signal" and "PU signal transmitted," respectively. The detection probability $P_d \triangleq P(Y > \gamma|\mathcal{H}_1)$ is affected only by the event $\mathcal{I}$ [7], since if the event $\mathcal{O}$ occurs, the CR user cannot sense the PU. Instead, the false-alarm probability $P_f \triangleq P(Y > \gamma|\mathcal{H}_0)$ is affected by both the events $\mathcal{I}$ and $\mathcal{O}$. Specifically:

$$\begin{aligned} P_d &= P(Y > \gamma|\mathcal{H}_1,\mathcal{I})P(\mathcal{I}) + \underbrace{P(Y > \gamma|\mathcal{H}_1,\mathcal{O})}_{=0} P(\mathcal{O}) = \\ &= P(Y > \gamma|\mathcal{H}_1,\mathcal{I})P(\mathcal{I}) \end{aligned} \tag{24}$$

$$\begin{aligned} P_f &= P(Y > \gamma|\mathcal{H}_0,\mathcal{I})P(\mathcal{I}) + P(Y > \gamma|\mathcal{H}_0,\mathcal{O})P(\mathcal{O}) \geq \\ &\geq P(Y > \gamma|\mathcal{H}_0,\mathcal{I})P(\mathcal{I}) \end{aligned} \tag{25}$$

with $P(\mathcal{I}) = \overline{\mathcal{S}}/\overline{\mathcal{T}}$. From (24) and (25), it results that observing the band for a time greater than the average sojourn time $\overline{\mathcal{S}}$ has two effects: i) P_d does not improve; ii) P_f can increase[6]. Hence, for an efficient spectrum sensing, T_{s} has to be set by accounting only for $\overline{\mathcal{S}}$. ■

The result (23) agrees with the intuition: if the event $\mathcal{O}$ occurs, the CR user can use the band without interfering the PU. So, it is useless to waste time by sensing a free band.

Insight 2 (Optimal Mobility-Aware Sensing Threshold)**.** From Prop. 4 and according to Def. 11, the optimal sensing time threshold is equal to the average PU sojourn time $\overline{\mathcal{S}}$.

Insight 3 (Mobility-Aware Sensing Time)**.** The amount $\nu_{(P_d,P_f)}$ of the average sojourn time to be devoted to the

[6]We observe that, when T_{s} is perfectly divided between the events $\mathcal{I}$ and $\mathcal{O}$, $P_f = P(Y > \gamma|\mathcal{H}_0,\mathcal{I}) = P(Y > \gamma|\mathcal{H}_0,\mathcal{O})$.

sensing depends on the required detection accuracy (P_d, P_f) and on the adopted sensing technique. Consequently, (23) can be rewritten as follows:

$$\begin{aligned} T_{\rm s} &= \nu_{(P_d,P_f)}\,\overline{S} = \nu_{(P_d,P_f)}\,P(\mathcal{I})\,\overline{\mathcal{T}} = \\ &= \nu_{(P_d,P_f)}\,\frac{P(\mathcal{I})}{1-P(\mathcal{I})}\,\overline{\Theta}, \quad \nu_{(P_d,P_f)} \in (0,1] \end{aligned} \tag{26}$$

where $\nu_{(P_d,P_f)}$ accounts for the targeted detection accuracy (P_d, P_f) and the adopted sensing technique characteristics. Moreover, in the last two equality of (26), we have used (8) and Theorem 1. (26) provides a practical rule for setting $T_{\rm s}$ according to the mobile PU dynamics.

Remark 7. If $\overline{S} \to 0$, $T_{\rm s} \to 0$ as well. This agrees with the intuition: if the PU is never in the CR interference region, it is useless to sense the band. If $\overline{\Theta} \to 0$, i.e., if the PU is always in the CR interference region, $T_{\rm s}$ has to be set according to the static scenario rules.

D. Mobility-Aware Sensing Time for RWM and RWPM

In the following, we specialize (26) for both the considered mobility models.

Theorem 5. *When a PU is roaming within a network region $\boldsymbol{A}$ according to the RWM, the sensing time $T_{s\text{-}RWM}$ of an arbitrary CR user must be set as follows:*

$$T_{s\text{-}RWM} = \nu_{(P_d,P_f)}\,\frac{P_{RWM}(\mathcal{I})}{1-P_{RWM}(\mathcal{I})}\,\overline{\Theta}_{RWM} = \tag{27}$$
$$\begin{cases} \dfrac{a\,\nu_{(P_d,P_f)}\left[2\left(\frac{R}{a}\right)-\left(\frac{R}{a}\right)^2\right]}{\overline{v}_{RWM}\left[1-2\left(\frac{R}{a}\right)+\left(\frac{R}{a}\right)^2\right]}, & A=[0,a] \\ \dfrac{a^2\nu_{(P_d,P_f)}\left[\pi\left(\frac{R}{a}\right)^2-\frac{8}{3}\left(\frac{R}{a}\right)^3+\frac{1}{2}\left(\frac{R}{a}\right)^4\right]}{2\,R\,\overline{v}_{RWM}\left[1-\left(\pi\left(\frac{R}{a}\right)^2-\frac{8}{3}\left(\frac{R}{a}\right)^3+\frac{1}{2}\left(\frac{R}{a}\right)^4\right)\right]}, & \boldsymbol{A}=[0,a]\times[0,a] \end{cases}$$

Proof: By substituting (10) in (26), and by accounting for the expression of $P_{\rm RWM}(\mathcal{I})$ in both one-dimensional and bi-dimensional network region [7], (27) is obtained. ∎

Corollary 1. *When a PU is roaming within a network region $\boldsymbol{A}$ according to the RWM and $R << a$, the sensing time $T_{s\text{-}RWM}$ can be approximated as follows:*

$$T_{s\text{-}RWM} = \begin{cases} \dfrac{2\,R\,a\;\nu_{(P_d,P_f)}}{\overline{v}_{RWM}(a-2\,R)}, & A=[0,a] \\ \dfrac{\pi\,R\,a^2\;\nu_{(P_d,P_f)}}{2\,\overline{v}_{RWM}(a^2-\pi\,R^2)}, & \boldsymbol{A}=[0,a]\times[0,a] \end{cases} \tag{28}$$

Proof: (28) is immediately obtained by evaluating (27) when $R/a \to 0$. ∎

Theorem 6. *When a PU is roaming within a network region $\boldsymbol{A}$ according to the RWPM, the sensing time $T_{s\text{-}RWPM}$ of an arbitrary CR user must be set as follows:*

$$T_{s\text{-}RWPM} = \nu_{(P_d,P_f)}\,\frac{P_{RWPM}(\mathcal{I})}{1-P_{RWPM}(\mathcal{I})}\,\overline{\Theta}_{RWPM} = \tag{29}$$
$$\begin{cases} \dfrac{2\,a\,\nu_{(P_d,P_f)}\tanh^{-1}\left(1-\frac{\overline{L}}{a}\right)\left[2\left(\frac{R}{a}\right)-2\left(\frac{R}{a}\right)^3+\left(\frac{R}{a}\right)^4\right]}{3\,\overline{v}_{RWPM}\left[1-\left(2\left(\frac{R}{a}\right)-2\left(\frac{R}{a}\right)^3+\left(\frac{R}{a}\right)^4\right)\right]}, & A=[0,a] \\ \dfrac{\pi\left(\frac{R}{a}\right)^2-\frac{3\pi}{2}\left(\frac{R}{a}\right)^4+\frac{32}{15}\left(\frac{R}{a}\right)^5+\frac{3\pi}{8}\left(\frac{R}{a}\right)^6-\frac{32}{35}\left(\frac{R}{a}\right)^7+\frac{1}{6}\left(\frac{R}{a}\right)^8}{\left[1-\left(\pi\left(\frac{R}{a}\right)^2-\frac{3\pi}{2}\left(\frac{R}{a}\right)^4+\frac{32}{15}\left(\frac{R}{a}\right)^5+\frac{3\pi}{8}\left(\frac{R}{a}\right)^6-\frac{32}{35}\left(\frac{R}{a}\right)^7+\frac{1}{6}\left(\frac{R}{a}\right)^8\right)\right]} & \\ \dfrac{2\,a^2\,\nu_{(P_d,P_f)}\tanh^{-1}\left(1-\frac{\overline{L}}{a}\right)\tanh^{-1}\left(1-\frac{2R}{a}\right)}{9\,R\,\overline{v}_{RWPM}}, & \boldsymbol{A}=[0,a]\times[0,a] \end{cases}$$

Proof: By substituting (13) in (26) and by accounting for the expression of $P_{\rm RWPM}(\mathcal{I})$ in both one-dimensional and bi-dimensional network region [7], (29) is obtained. ∎

Corollary 2. *When a PU is roaming within a network region $\boldsymbol{A}$ according to the RWPM and $R << a$, the sensing time $T_{s\text{-}RWPM}$ can be approximated as follows:*

$$T_{s\text{-}RWPM} = \begin{cases} \dfrac{4\,a\,\nu_{(P_d,P_f)}R\tanh^{-1}\left(1-\frac{\overline{L}}{a}\right)}{3\,\overline{v}_{RWPM}(a-2\,R)}, & A=[0,a] \\ \dfrac{2\,\pi\,R\,a^2\nu_{(P_d,P_f)}}{9\,\overline{v}_{RWPM}} & \\ \dfrac{\tanh^{-1}\left(1-\frac{\overline{L}}{a}\right)\tanh^{-1}\left(1-\frac{2R}{a}\right)}{(a^2-\pi\,R^2)}, & \boldsymbol{A}=[0,a]\times[0,a] \end{cases} \tag{30}$$

Proof: (30) is immediately obtained by evaluating (29) when $R/a \to 0$. ∎

Remark 8. (27) and (29) provide practical rules for setting $T_{\rm s}$ according to the PU mobility patterns, and they prove that $T_{\rm s}$ depends on four factor: i) the normalized PU protection range R/a; ii) the extension of the network region $\boldsymbol{A}$; iii) the average PU velocity; iv) the sensing accuracy $\nu_{(P_d,P_f)} \in (0,1]$.

E. Mobility-Aware Sensing Efficiency

In this subsection, we analytically evaluate a lower bound of the sensing efficiency achievable by a CR user on a targeted spectrum band in presence of PU mobility.

Proposition 5. *The mobility-aware sensing efficiency $\eta_{mob} \triangleq \frac{T_{Tx}^{opt}}{T_{sp}}$, achievable by a CR user when the PU moves according to the RWM or the RWMP, satisfies the following inequality:*

$$\begin{aligned} \eta_{mob} &= 1 - \frac{1}{1+\frac{T_{Tx}^{opt}}{\nu_{(P_d,P_f)}\frac{P(\mathcal{I})}{1-P(\mathcal{I})}\Theta}} \geq \\ &\geq \begin{cases} 1-\dfrac{1}{1+\frac{\log\left(\frac{P_{on}}{P_{on}-P_{int}}\right)}{\nu_{(P_d,P_f)}}\frac{1-P_{RWM}(\mathcal{I})}{P_{RWM}(\mathcal{I})}}, & RWM \\ 1-\dfrac{1}{1+\frac{\log\left(\frac{P_{on}}{P_{on}-P_{int}}\right)}{\nu_{(P_d,P_f)}\,\varphi\left(\overline{L},R,a\right)}\frac{1-P_{RWPM}(\mathcal{I})}{P_{RWPM}(\mathcal{I})}}, & RWPM \end{cases} \end{aligned} \tag{31}$$

where $T_{sp} \triangleq T_s + T_{Tx}^{opt}$ denotes the sensing period.

Proof: The proof follows by substituting (18), (20) and (26) in $\eta_{\rm mob}$. ∎

Remark 9. In mobile scenarios, the sensing efficiency (31) depends on three factors: i) the PU interference constraint; ii) the PU mobility model; iii) the PU traffic. $\eta_{\rm mob}$ reflects the

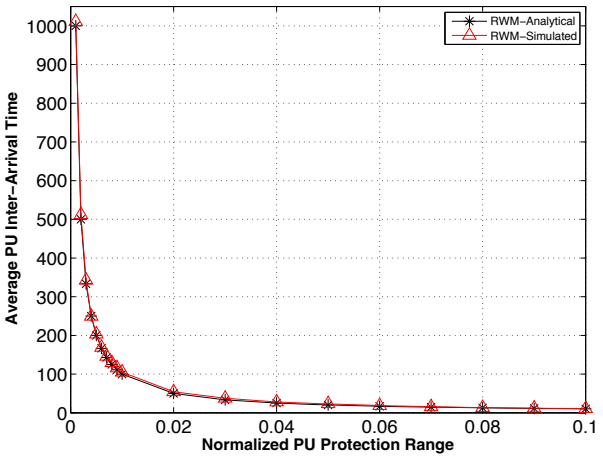

Fig. 3. $\overline{\mathcal{T}}_{\text{RWM}}$, $\frac{v_{\min}}{a} = 0.1$, $\frac{v_{\max}}{a} = 0.9$.

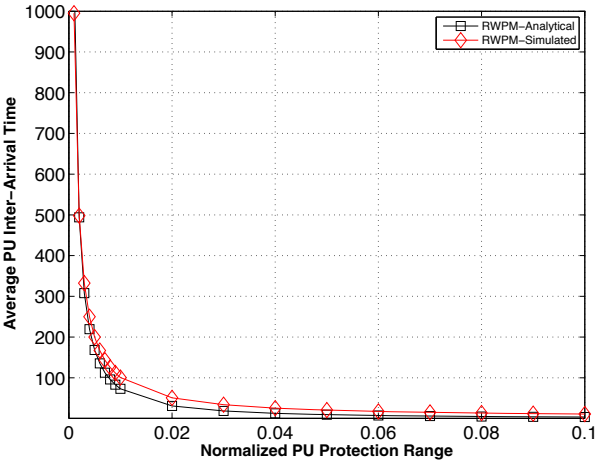

Fig. 4. $\overline{\mathcal{T}}_{\text{RWPM}}$, $\frac{v_{\min}}{a} = 0.1$, $\frac{v_{\max}}{a} = 0.9$.

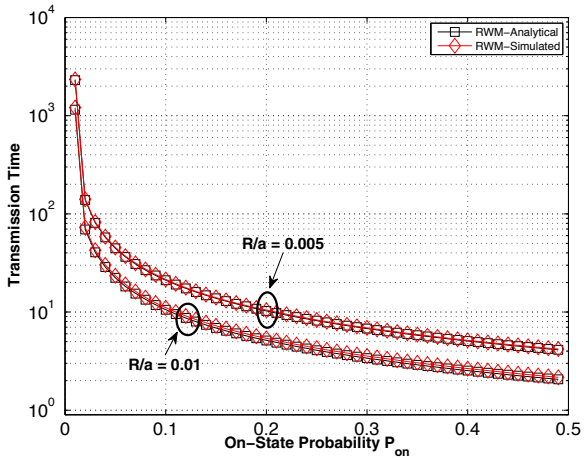

Fig. 5. $T^{\text{opt}}_{\text{Tx-RWM}}$, $P_{\text{int}} = 10^{-2}$, $\frac{v_{\min}}{a} = 0.1$, $\frac{v_{\max}}{a} = 0.9$.

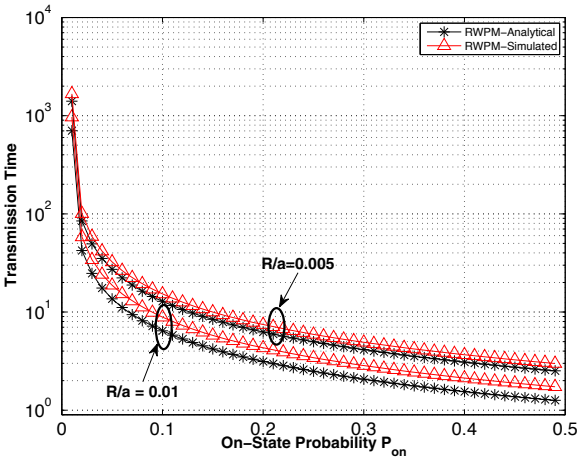

Fig. 6. $T^{\text{opt}}_{\text{Tx-RWPM}}$, $P_{\text{int}} = 10^{-2}$, $\frac{v_{\min}}{a} = 0.1$, $\frac{v_{\max}}{a} = 0.9$.

dynamic nature of both the PU topology through $P(\mathcal{I})$, and the PU traffic through P_{on}.

Remark 10. Given T_{s}, P_{int} and P_{on}, if the average PU out-time increases (e.g., the PU velocity decreases or R/a decreases), η_{mob} increases as well, since the CR user can use the band for a longer time by assuring the same P_{int}. Given P_{int}, $\overline{S}$ and $\overline{\Theta}$, if $P_{\text{on}} \to P_{\text{int}}$, $\eta_{\text{mob}} \to 1$. In fact, in such a case the CR user can transmit on a time interval arbitrarily long.

VI. Validation of the Theoretical Results

In this section, we validate the derived analytical results by Monte Carlo simulations. We generate 10^3 topologies by placing the CR users uniformly at random in a bi-dimensional network region $\boldsymbol{A}$. For each topology, the PU starts from its steady-state spatial distribution and then it moves according to the RWM or the RWPM for enough time to assure 10^6 inter-arrival events.

We first validate the results of Section IV. Figs. 3 and 4 show the average PU inter-arrival time $\overline{\mathcal{T}}$ versus the normalized PU protection range R/a. We set the normalized maximum and minimum PU velocity equal to $v_{\max}/a = 0.9$ and $v_{\min}/a = 0.1$, respectively. The analytical results (10) and (13) match well the simulation results for both the adopted mobility models. In particular, we note that the effects of the approximation we made in the proof to account for the edges are more evident in the RWPM than in the RWM, since the RWPM steady-state spatial distribution is not uniform.

We now validate the results of Section V. Figs. 5 and 6 show the optimal mobility-aware transmission time $T^{\text{opt}}_{\text{Tx}}$ as the PU on-state probability P_{on} increases, for both the adopted mobility models. We set $P_{\text{int}} = 10^{-2}$ and we consider two values of R/a, i.e., $R/a = 0.005$ and $R/a = 0.01$. The analytical results are obtained by setting $T^{\text{opt}}_{\text{Tx}}$ according to the lower bounds derived in Theorem 3 and Theorem 4. We note that the theoretical results match well the simulation results. In particular, when R/a increases, $T^{\text{opt}}_{\text{Tx}}$ decreases, since the probability of a CR user being inside the PU protection range increases. Moreover, $T^{\text{opt}}_{\text{Tx}}$ decreases when P_{on} increases. In fact, in such a case, the PU traffic dynamics increase.

Figs. 7 and 8 depict the instantaneous interference level produced by a CR user on the PU transmissions during the PU movements, when the transmission time is set according to Theorem 3 and Theorem 4, respectively. The results are obtained for $P_{\text{on}} = 1/3$, $P_{\text{int}} = 10^{-2}$ and $R/a = 0.005$. The horizontal red line in both the figures represents P_{int}. The results confirm the benefits of setting the transmission time according to the theoretical results. In particular, the

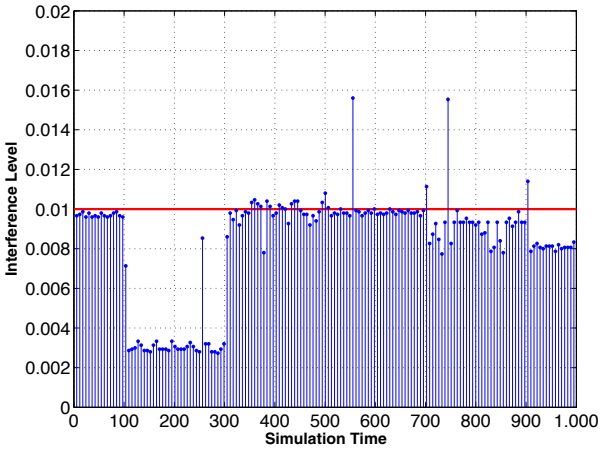

Fig. 7. Interference-Level RWM, $P_{\text{int}} = 10^{-2}$, $P_{\text{on}} = \frac{1}{3}$.

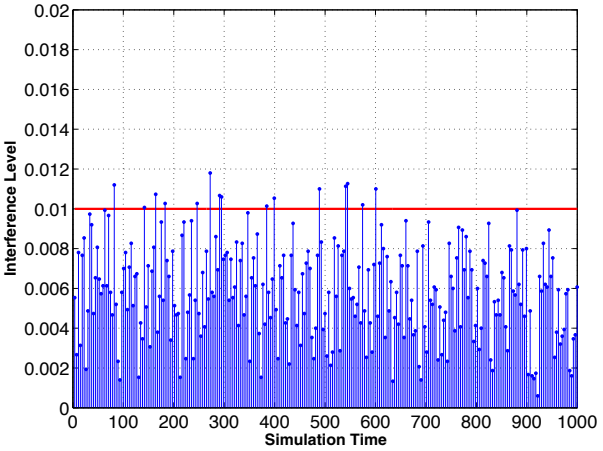

Fig. 8. Interference-Level RWPM, $P_{\text{int}} = 10^{-2}$, $P_{\text{on}} = \frac{1}{3}$.

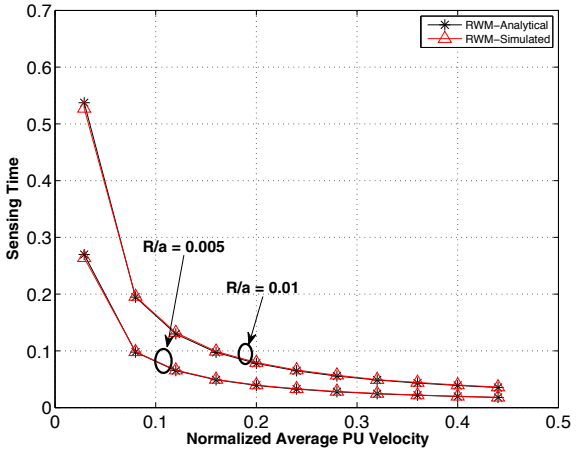

Fig. 9. $T_{\text{s-RWM}}$, $\frac{R}{a} = 0.005$ and $\frac{R}{a} = 0.01$

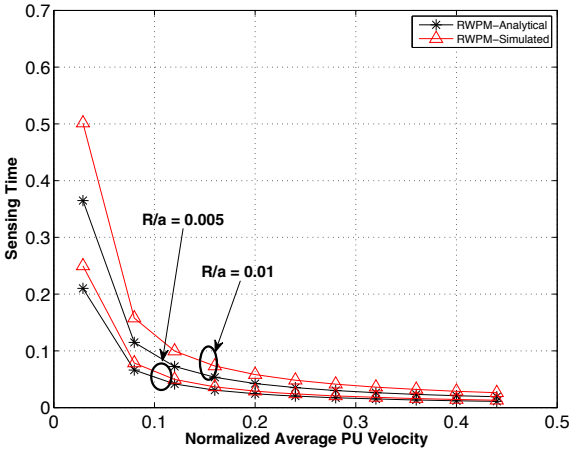

Fig. 10. $T_{\text{s-RWPM}}$, $\frac{R}{a} = 0.005$ and $\frac{R}{a} = 0.01$

average interference levels (obtained by averaging the instantaneous interference level over the simulation time) on the PU transmissions for the RWM and for the RWPM are equal to $9 \cdot 10^{-3} < P_{\text{int}}$ and $6 \cdot 10^{-3} < P_{\text{int}}$, respectively. We note that the shape of the interference level in the RWM is due to the constant duration of each movement.

Figs. 9 and 10 report the sensing time T_{s} versus the normalized average PU velocity for both the adopted mobility models, when $R/a = 0.005$ and $R/a = 0.01$. The analytical results are obtained by setting T_{s} according to Theorem 5 and Theorem 6, with $\nu_{(P_d,P_f)} = 1$. We note that the theoretical results match well the simulation results. In particular, when R/a increases, T_{s} increases as well, since the probability of a CR user being inside the PU protection range increases. Moreover, T_{s} decreases when the normalized average PU velocity increases, since the time the PU spends inside the CR interference region decreases.

Fig. 11 shows the false-alarm probability P_f as the sensing time T_{s} increases, i.e., as the number $N = T_{\text{s}}\, f_s$ [3] of samples collected by the CR user during T_{s} increases (f_s denotes the sampling frequency). The results are obtained by adopting the classical energy detector with $SNR = -5$ dB and for a fixed value of the detection probability $P_d = 0.999$. Two values of the average PU sojourn time $\overline{\mathcal{S}}$ are considered, i.e., $N_{\overline{\mathcal{S}}} = \overline{\mathcal{S}}\, f_s = 100$ and $N_{\overline{\mathcal{S}}} = \overline{\mathcal{S}}\, f_s = 200$. The results validate the analysis developed in Section V. In fact, for sensing times longer than $\overline{\mathcal{S}}$, P_f increases, confirming so the presence of a threshold behavior for the sensing accuracy.

VII. Discussion

Here, we discuss the derived results along with some directions for future research.

Our work aims at revising the current design of the spectrum sensing functionality for jointly maximizing the sensing efficiency and satisfying the PU interference constraint in presence of PU mobility. Specifically, we answer two fundamental questions: i) How often must the sensing be performed in presence of PU mobility? ii) How long must a spectrum band be sensed to reliably detect mobile PUs?

The theoretical analysis carried out through the paper reveals that:

- For a realistic deployment of the CR paradigm in mobile PU scenarios, *it is mandatory to tune the sensing and the transmission times according to the mobile PU dynamics*, regardless of the challenges that might be faced to catch the mobility characteristics of the PU network. In fact, as shown in Section II and in Section V, tuning the

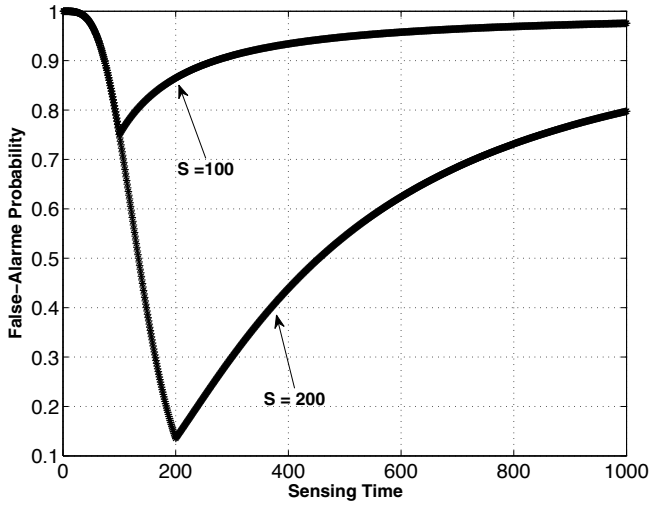

Fig. 11. $P_d = 0.999$, SNR$= -5$dB.

sensing and the transmission times according only to the traditional static-scenario factors does not assure PU interference avoidance and sensing efficiency.

- The optimal mobility-aware sensing and transmission times, derived in this paper, exhibit a very attractive and powerful feature: *they do not depend on the instantaneous values of the PU mobility pattern but only on the average statistics*, such as the average PU sojourn time and the average PU out time.

Regarding the aforementioned average statistics needed for the optimal mobility-aware spectrum sensing design, we observe that:

- The statistics of the PU mobility pattern can be obtained through measurement campaigns. Over the past years, a large amount of mobility traces have become available, and they have been extensively analyzed to extract the average statistics of real-world mobility [16], [17]. Clearly, further research is needed to assess the relevance of the available mobility traces in CR scenarios.
- The statistics of the PU mobility pattern can be directly provided to the CR users by the PU network. In fact, in some applications, as for example military CR networks, the PUs may be motivated to cooperate with CR users [1]. Further research is needed to design effective models for the cooperation between the CR and the PU networks.

We further observe that, among the several CR scenarios in which the PUs are mobile and, hence, the proposed mobility-aware spectrum sensing design must be adopted, the small-scale PU networks[7] have recently gained attention in the CR literature [1], [11]. However, a reliable and effective application of the CR paradigm in these scenarios is still an open problem. In particular, further research is needed to assess the effects of the mobility on the spectrum sensing functionality when both the CR users and the PUs are mobile.

[7]Examples of small-scale PU networks include ad hoc networks, wireless personal area networks, and wireless microphones.

VIII. Conclusions

In this paper, an optimal spectrum sensing design for Cognitive Radio networks in presence of Primary User (PU) mobility has been proposed. A theoretical analysis has been developed to determine the optimal values for both the transmission and the sensing times, with reference to a general PU mobility model. Regarding the transmission time, a closed-form expression of the optimal value that jointly maximizes the spectrum sensing efficiency and satisfies the PU interference constraint has been derived. Regarding the sensing time, it has been proved that, in mobile scenario, the sensing accuracy exhibits a threshold behavior as a function of the sensing time, and the closed-form expression of the threshold has been determined.

Then, the theoretical results have been specialized for two widely adopted mobility models. Finally, practical rules for the sensing parameter tuning have been provided with reference to the considered mobility models. The analytical results have been validated through simulations.

Appendix A
Proof of Proposition 1

We use techniques similar to those used in [18]. Let us consider a CR user at a location $\boldsymbol{x}_{\text{CR}} \in \boldsymbol{A}$. The mobile PU meets the CR user during a movement of length $L = l_i$, if the PU enters in the CR interference region. The probability of this event is $P_{\boldsymbol{C}(\boldsymbol{x}_{\text{CR}},l_i)} = \int_{\boldsymbol{C}(\boldsymbol{x}_{\text{CR}},l_i)} f_{\boldsymbol{X}_{\text{PU}}}(\boldsymbol{x}_{\text{PU}}) d\boldsymbol{x}_{\text{PU}}$. Hence, the probability that the CR user has not been encountered after k movement periods is: $P(\mathcal{M} > k|\boldsymbol{x}_{\text{CR}}) = \int_{\mathcal{L}_1} \dots \int_{\mathcal{L}_k} (1 - P_{\boldsymbol{C}(\boldsymbol{x}_{\text{CR}},l_1)}) \dots (1 - P_{\boldsymbol{C}(\boldsymbol{x}_{\text{CR}},l_k)}) f_{L_1 \dots L_k}(l_1, \dots, l_k) dl_1 \dots dl_k$. Although the lengths of consecutive movements are not independent, by using Assumption 1 and by reasoning as in [14], the length process can be assumed ergodic. Thus, the analysis can be simplified by considering the lengths independent:

$$P(\mathcal{M} > k|\boldsymbol{x}_{\text{CR}}) = \left(1 - \int_{\mathcal{L}} P_{\boldsymbol{C}(\boldsymbol{x}_{\text{CR}},l)} f_L(l) dl\right)^k \quad (32)$$

Hence, the CDF of the r.v. $\mathcal{M}$ conditioned to $\boldsymbol{x}_{\text{CR}}$ is geometric with success probability $P_g(\boldsymbol{x}_{\text{CR}}) \triangleq \int_{\mathcal{L}} P_{\boldsymbol{C}(\boldsymbol{x}_{\text{CR}},l)} f_L(l)\, dl$. Consequently, $E[\mathcal{M}|\boldsymbol{x}_{\text{CR}}] = (P_g(\boldsymbol{x}_{\text{CR}}))^{-1}$.

Appendix B
Proof of Proposition 2

According to Def. 5 and without loss of generality, $\Theta = t - t_1$. It is useful to express Θ as function of the r. v. $\mathcal{M}$, i.e., $\Theta = t - t_1 = \sum_{l=1}^{\mathcal{M}} D_l + \xi - t_1$, where D_l is the movement duration (see Def. 4) and $\xi \triangleq t - \sum_{l=1}^{\mathcal{M}} D_l$ denotes the not-integer part of the $(\mathcal{M}+1)$-th period. Hence

$$\overline{\Theta} \triangleq E[\Theta] = \sum_{k=1}^{+\infty} E\left[\Theta|\mathcal{M} = k\right] P(\mathcal{M} = k) = \overline{D}\,\overline{\mathcal{M}} \quad (33)$$

(33) accounts for the identical distribution of ξ and t_1 (Assumption 1). By integrating $E[\mathcal{M}|\boldsymbol{x}_{\text{CR}}]$ over all the CR user locations and by substituting in (33), the result (5) is proved:

$$\overline{\Theta} = \overline{D} \int_{\boldsymbol{A}} \frac{f_{\boldsymbol{X}_{\text{CR}}}(\boldsymbol{x}_{\text{CR}}) d\boldsymbol{x}_{\text{CR}}}{\int_{\mathcal{L}} \int_{\boldsymbol{C}(\boldsymbol{x}_{\text{CR}},l)} f_{\boldsymbol{X}_{\text{PU}}}(\boldsymbol{x}_{\text{PU}}) d\boldsymbol{x}_{\text{PU}}\, f_L(l) dl} \tag{34}$$

APPENDIX C
PROOF OF THEOREM 2

By using (3), it results $P(\mathcal{T} > t) = P(\mathcal{S} + \Theta > t) \geq P(\Theta > t) \geq P\left(\sum_{l=1}^{\mathcal{M}-1} D_l > t\right)$. Since $\mathcal{M}|\boldsymbol{x}_{\text{CR}}$ is a geometric r.v., and $\{D_l\}$ are i.i.d. non-negative random variables, if $P_g(\boldsymbol{x}_{\text{CR}})$ is sufficient small (i.e. $R << a$), by applying the Rényi Theorem [19], the proof follows:

$$P(\mathcal{T} \leq t) \leq \int_{\boldsymbol{A}} P\left(\sum_{l=1}^{\mathcal{M}-1} D_l \leq t | \boldsymbol{x}_{\text{CR}}\right) f_{\boldsymbol{X}_{\text{CR}}}(\boldsymbol{x}_{\text{CR}}) d\boldsymbol{x}_{\text{CR}} \simeq$$
$$\simeq 1 - \int_{\boldsymbol{A}} e^{-\frac{t\, P_g(\boldsymbol{x}_{\text{CR}})}{D}} f_{\boldsymbol{X}_{\text{CR}}}(\boldsymbol{x}_{\text{CR}}) d\boldsymbol{x}_{\text{CR}} \tag{35}$$

APPENDIX D
THEOREM 1 FOR RWM AND THEOREM 2 FOR RWM

Theorem 1 for RWM : We neglect the boarder effects, i.e., we suppose $R << a$. For the RWM, $f_{\boldsymbol{X}_{\text{PU}}}(\boldsymbol{x}_{\text{PU}}) = f_{X_{\text{PU}} Y_{\text{PU}}}(x_{\text{PU}}, y_{\text{PU}})$ is uniform [13], hence:

$$P_g(\boldsymbol{x}_{\text{CR}}) = \int_{\mathcal{L}} P_{\boldsymbol{C}(\boldsymbol{x}_{\text{CR}},l)}\, f_L(l) dl \simeq$$
$$\simeq \begin{cases} \frac{\overline{L}}{a}, & A = [0, a] \\ \frac{2\, R\, \overline{L}}{a^2}, & \boldsymbol{A} = [0, a] \times [0, a] \end{cases} \tag{36}$$

where $\overline{L} \triangleq E[L]$ is the average value of the r.v. L, equal to[8] $\overline{L} = \overline{D}\, \overline{v}_{\text{RWM}}$, with $\overline{v}_{\text{RWM}} = \frac{v_{\max} + v_{\min}}{2}$. By substituting (36) in (6), and by using the CR uniform spatial distribution, we have:

$$\overline{\mathcal{T}}_{\text{RWM}} = \begin{cases} \frac{a}{\overline{v}_{\text{RWM}}(1 - P_{\text{1D-RWM}}(\mathcal{I}))}, & A = [0, a] \\ \frac{a^2}{2\, R\, \overline{v}_{\text{RWM}}(1 - P_{\text{2D-RWM}}(\mathcal{I}))}, & \boldsymbol{A} = [0, a] \times [0, a] \end{cases} \tag{37}$$

where $P_{\text{1D-RWM}}(\mathcal{I})$ and $P_{\text{2D-RWM}}(\mathcal{I})$ [7] are reported in *Theorem 1 for RWM* for the sake of completeness. The derived $\overline{\Theta}_{\text{2D-RWM}} = \overline{\mathcal{T}}_{\text{2D-RWM}}(1 - P_{\text{2D-RWM}}(\mathcal{I}))$ coincides with the hitting time expression derived in [18] for the Random Direction mobility Model (RDM). In fact, both the RWM and the RDM are characterized by a uniform spatial distribution.

Theorem 2 for RWM: By substituting (36) and $\overline{D} = \frac{\overline{L}}{\overline{v}_{\text{RWM}}}$ in (9), the proof is accomplished:

$$P(\mathcal{T}_{\text{RWM}} \leq t) \leq 1 - e^{-\frac{t}{\overline{\Theta}_{\text{RWM}}}} \triangleq 1 - e^{-\Omega_{\text{RWM}}\, t} \tag{38}$$

[8]According to the RWM (Section IV-B), each movement occurs in a constant time, hence $\overline{D} = D = \text{const}$.

APPENDIX E
THEOREM 1 FOR RWPM AND THEOREM 2 FOR RWPM

Theorem 1 for RWPM: As for the RWM, we suppose $R << a$. For the RWPM, $f_{\boldsymbol{X}_{\text{PU}}}(\boldsymbol{x}_{\text{PU}})$ is not uniform, hence, by substituting the expressions of $f_{\boldsymbol{X}_{\text{PU}}}(\boldsymbol{x}_{\text{PU}})$ [14] in $P_g(\boldsymbol{x}_{\text{CR}})$, one has:

$$P_g(\boldsymbol{x}_{\text{CR}}) = \int_{\mathcal{L}} P_{\boldsymbol{C}(\boldsymbol{x}_{\text{CR}},l)}\, f_L(l) dl \simeq$$
$$\simeq \begin{cases} \frac{6\, x_{\text{CR}}\left(1 - \frac{x_{\text{CR}}}{a}\right)\overline{L}}{a^2}, & A = [0, a] \\ \frac{72\, R\, \overline{L}\, x_{\text{CR}}\, y_{\text{CR}}\left(1 - \frac{x_{\text{CR}}}{a}\right)\left(1 - \frac{y_{\text{CR}}}{a}\right)}{a^4}, & \boldsymbol{A} = [0, a] \times [0, a] \end{cases} \tag{39}$$

where $\overline{L} \triangleq E[L]$ is the average movement length. In the RWPM (Section IV-C), the r.v. D is obtained as random function of the two random variables L and v, and its average value is given by $\overline{D} = \frac{\overline{L}\, \log(v_{\max}/v_{\min})}{v_{\max} - v_{\min}}$ [14]. By denoting with $\overline{v}_{\text{RWPM}}$ the quantity[9] $\frac{v_{\max} - v_{\min}}{\log(v_{\max}/v_{\min})}$, it results $\overline{D} = \frac{\overline{L}}{\overline{v}_{\text{RWPM}}}$. By substituting (39) in (6), by using the expression of $\overline{D}$ and the notable equality $\int 1/(b^2 - u^2) du = \tanh^{-1}(u/\sqrt{b}) + cost$, after some manipulations we obtain:

$$\overline{\mathcal{T}}_{\text{RWPM}} = \begin{cases} \frac{2a \tanh^{-1}\left(1 - \frac{\overline{L}}{a}\right)}{3\, \overline{v}_{\text{RWPM}}(1 - P_{\text{1D-RWPM}}(\mathcal{I}))}, & A = [0, a] \\ \frac{2a^2 \tanh^{-1}\left(1 - \frac{\overline{L}}{a}\right) \tanh^{-1}\left(1 - \frac{2R}{a}\right)}{9 R\, \overline{v}_{\text{RWPM}}(1 - P_{\text{2D-RWPM}}(\mathcal{I}))}, & \boldsymbol{A} = [0, a] \times [0, a] \end{cases} \tag{40}$$

with $P_{\text{1D-RWPM}}(\mathcal{I})$ and $P_{\text{2D-RWPM}}(\mathcal{I})$ [7] reported in *Theorem 1 for RWPM* for the sake of completeness.

Theorem 2 for RWPM: It is useful to distinguish between the one-dimensional and the bi-dimensional case.

• One-dimensional network region $A = [0, a]$:

By substituting (39) in (9), and by using the notable equality $\int e^{-(qz^2 + 2bz + c)} dz = 1/2 \sqrt{\pi/q}\, e^{\frac{b^2 - qc}{q}} \text{erf}(\sqrt{q} z + b/\sqrt{q}) + \text{const}$ [15], one has:

$$P(\mathcal{T}_{\text{RWPM}} \leq t) \leq 1 - {}_1F_1\left(\frac{1}{2}; \frac{3}{2}; \frac{3\overline{v}_{\text{RWPM}}}{2\, a} t\right) e^{-\frac{3\overline{v}_{\text{RWPM}}\, t}{2\, a}} \tag{41}$$
$$\leq 1 - e^{-\Psi_{\text{1D-RWPM}} t}$$

where ${}_1F_1(d; f; u) = \frac{\sqrt{\pi}}{2} \frac{\text{erfi}(\sqrt{u})}{\sqrt{u}}$ is the Kummer confluent hypergeometric function [15] and $\text{erfi}(u) \triangleq -i\, \text{erf}(i\, u)$ is the imaginary error function. In the last inequality of (41), we used the property ${}_1F_1(d; f; u) \geq 1$, which holds when u is a positive real number and we denoted with $\Psi_{\text{1D-RWPM}} \triangleq \frac{3\overline{v}_{\text{RWPM}}}{2\, a} = \tanh^{-1}\left(1 - \frac{\overline{L}}{a}\right) / \overline{\Theta}_{\text{1D-RWPM}}$. Moreover, since $\lim_{u \to 0} {}_1F_1(d; f; u) = 1$ and $\lim_{u \to \infty} {}_1F_1(d; f; u)\, e^{-u} = 0$, we have: $1 - {}_1F_1\left(\frac{1}{2}; \frac{3}{2}; \frac{3\overline{v}_{\text{RWPM}}}{2\, a} t\right) e^{-\frac{3\overline{v}_{\text{RWPM}}}{2\, a} t} =$
$\begin{cases} 1 - e^{-\frac{3\overline{v}_{\text{RWPM}} t}{2\, a}}, & \frac{\overline{v}_{\text{RWPM}} t}{a} \to 0 \\ 1, & \frac{\overline{v}_{\text{RWPM}} t}{a} \to \infty. \\ 1 - {}_1F_1\left(\frac{1}{2}; \frac{3}{2}; \frac{3\overline{v}_{\text{RWPM}} t}{2\, a}\right) e^{-\frac{3\overline{v}_{\text{RWPM}} t}{2\, a}}, & \text{otherwise} \end{cases}$

• Bi-dimensional network region $\boldsymbol{A} = [0, a] \times [0, a]$:

By reasoning as for the one-dimensional case, by substituting

[9]Clearly, $\overline{v}_{\text{RWPM}}$ is function of the average value of the uniform r.v. modeling the PU velocity. In the paper, we refer to $\overline{v}_{\text{RWPM}}$ as average PU velocity for the sake of simplicity.

(39) in (9) and by defining $\Psi_{\text{2D-RWPM}} \triangleq 9\,R\overline{v}_{\text{RWPM}}/(2\,a^2) = \tanh^{-1}\left(1-\frac{\overline{L}}{a}\right)\tanh^{-1}\left(1-\frac{2\,R}{a}\right)/\overline{\Theta}_{\text{2D-RWPM}}$, one has:

$$P(\mathcal{T}_{\text{RWPM}} \leq t) \leq 1 - \frac{1}{a}\int_0^a {}_1F_1\left(\frac{1}{2};\frac{3}{2};18\,R\,t\,\frac{\overline{v}_{\text{RWPM}}(a x_{\text{CR}} - x_{\text{CR}}^2)}{a^4}\right) e^{-\frac{18\,R\,t\,\overline{v}_{\text{RWPM}}(a x_{\text{CR}} - x_{\text{CR}}^2)}{a^4}} dx_{\text{CR}} \leq \tag{42}$$

$$\leq 1 - {}_1F_1\left(\frac{1}{2};\frac{3}{2};\frac{9\,R\overline{v}_{\text{RWPM}}}{2\,a^2}t\right) e^{-\frac{9\,R\overline{v}_{\text{RWPM}}}{2\,a^2}t}$$

$$\leq 1 - e^{-\Psi_{\text{2D-RWPM}}t}$$

with $1 - {}_1F_1\left(\frac{1}{2};\frac{3}{2};\frac{9\,R\overline{v}_{\text{RWPM}}t}{2\,a^2}\right) e^{-\frac{9\,R\overline{v}_{\text{RWPM}}t}{2\,a^2}} =$

$$\begin{cases} 1 - e^{-\frac{9\,R\overline{v}_{\text{RWPM}}t}{2\,a^2}}, & \frac{R\overline{v}_{\text{RWPM}}t}{a^2} \to 0 \\ 1, & \frac{R\overline{v}_{\text{RWPM}}t}{a^2} \to \infty \\ 1 - {}_1F_1\left(\frac{1}{2};\frac{3}{2};\frac{9\,R\overline{v}_{\text{RWPM}}t}{2\,a^2}\right) e^{-\frac{9\,R\overline{v}_{\text{RWPM}}t}{2\,a^2}}, & \text{otherwise} \end{cases}$$

ACKNOWLEDGEMENT

We thank Dr. M. Caleffi for his valuable feedback which helped us to improve the paper.

REFERENCES

[1] I. F. Akyildiz, B. F. Lo, and R. Balakrishnan, "Cooperative spectrum sensing in cognitive radio networks: A survey," *J. Physical Commun. (Elsevier)*, vol. 4, pp. 40–62, Mar. 2011.

[2] W.-Y. Lee and I. Akyildiz, "Optimal spectrum sensing framework for cognitive radio networks," *IEEE Trans. Wireless Commun.*, vol. 7, no. 10, pp. 3845–3857, Oct. 2008.

[3] Y.-C. Liang, Y. Zeng, E. C. Peh, and A. T. Hoang, "Sensing-throughput tradeoff for cognitive radio networks," *IEEE Trans. Wireless Commun.*, vol. 7, no. 4, pp. 1326–1337, Apr. 2008.

[4] W. Zhang, R. Mallik, and K. Letaief, "Optimization of cooperative spectrum sensing with energy detection in cognitive radio networks," *IEEE Trans. Wireless Commun.*, vol. 8, no. 12, pp. 5761–5766, Dec. 2009.

[5] E. Peh, Y.-C. Liang, Y. L. Guan, and Y. Zeng, "Power control in cognitive radios under cooperative and non-cooperative spectrum sensing," *IEEE Trans. Wireless Commun.*, vol. 10, no. 12, pp. 4238–4248, Dec. 2011.

[6] A. Ghasemi and E. S. Sousa, "Optimization of spectrum sensing for opportunistic spectrum access in cognitive radio networks," in *Proc. IEEE Consum. Commun. Netw. Conf. (CCNC)*, Jan. 2007, pp. 1022–1026.

[7] A. S. Cacciapuoti, I. F. Akyildiz, and L. Paura, "Primary-user mobility impact on spectrum sensing in cognitive radio networks," in *Proc. IEEE Symp. Personal, Indoor, Mobile Radio Commun. (PIMRC)*, Sep. 2011, pp. 451–456.

[8] T. Camp, J. Boleng, and V. Davies, "A survey of mobility models for ad hoc network research," *Wireless Commun. Mobile Computing*, vol. 2, no. 5, pp. 483–502, 2002.

[9] A. Min, K.-H. Kim, J. Singh, and K. Shin, "Opportunistic spectrum access for mobile cognitive radios," in *Proc. IEEE INFOCOM*, Apr. 2011, pp. 2993–3001.

[10] A. S. Cacciapuoti, I. F. Akyildiz, and L. Paura, "Correlation-aware user selection for cooperative spectrum sensing in cognitive radio ad hoc networks," *IEEE J. Sel. Areas Commun.*, vol. 30, no. 2, pp. 297–306, Feb. 2012.

[11] K. W. Choi, E. Hossain, and D. I. Kim, "Cooperative spectrum sensing under a random geometric primary user network model," *IEEE Trans. Wireless Commun.*, vol. 10, no. 6, pp. 1932–1944, June 2011.

[12] S. M. Ross, *Introduction to Probability Models*. Academic Press, 2000.

[13] J.-Y. L. Boudec and M. Vojnovic, "Perfect simulation and stationarity of a class of mobility models," in *Proc. IEEE INFOCOM*, Mar 2005, vol. 4.

[14] C. Bettstetter, H. Hartenstein, and X. Perez-Costa, "Stochastic properties of the random waypoint mobility model," *Wireless Netw.*, vol. 10, pp. 555–567, 2004.

[15] M. Abramowitz and I. Stegun, *Handbook of Mathematical Functions with Formulas, Graphs, and Mathematical Tables*. New York: Dover Publications, 1972.

[16] P. Hui, A. Chaintreau, J. Scott, R. Gass, J. Crowcroft, and C. Diot, "Pocket switched networks and human mobility in conference environments," in *Proc. ACM SIGCOMM Workshop Delay-tolerant Netw. (WDTN)*, 2005.

[17] J. Leguay, A. Lindgren, J. Scott, T. Friedman, and J. Crowcroft, "Opportunistic content distribution in an urban setting," in *Proc. ACM SIGCOMM Workshop Challenged Netw. (CHANTS)*, 2006.

[18] T. Spyropoulos, K. Psounis, and C. S. Raghavendra, "Performance analysis of mobility-assisted routing," in *Proc. ACM MobiHoc*, 2006.

[19] V. Kalashnikov, *Geometric Sums: Bounds for Rare Events with Applications*. Kluwer Academic Publishers, 1997.

Angela Sara Cacciapuoti received the Dr. Eng. degree summa cum laude in Telecommunications Engineering in 2005, and the Ph.D degree with score "excellent" in Electronic and Telecommunications Engineering in 2009, both from the University of Naples Federico II. Currently, she is an Assistant Professor with the Department of Electric Engineering and Information Technology (DIETI) at the University of Naples Federico II. From 2010 to 2011, Dr. Cacciapuoti was with the Broadband Wireless Networking Laboratory, Georgia Institute of Technology, as a visiting researcher. In 2011, she was also with the NaNoNetworking Center in Catalunya (N3Cat), Universitat Politècnica de Catalunya (UPC), as a visiting researcher. Her current research interests are in cognitive radio networks and non-stationary signal processing.

Ian F. Akyildiz received the B.S., M.S., and Ph.D. degrees in Computer Engineering from the University of Erlangen-Nürnberg, Germany, in 1978, 1981 and 1984, respectively. Currently, he is the Ken Byers Chair Professor in Telecommunications with the School of Electrical and Computer Engineering, Georgia Institute of Technology, Atlanta and the Director of the Broadband Wireless Networking Laboratory and Chair of the Telecommunication Group at Georgia Tech. Dr. Akyildiz is an honorary professor with the School of Electrical Engineering at Universitat Politècnica de Catalunya (UPC) in Barcelona, Catalunya, Spain, and the founder of N3Cat (NaNoNetworking Center in Catalunya). Since 2011, he is a Consulting Chair Professor at the Department of Information Technology, King Abdulaziz University (KAU) in Jeddah, Saudi Arabia. Since January 2013, Dr. Akyildiz is also a FiDiPro Professor (Finland Distinguished Professor Program (FiDiPro) supported by the Academy of Finland) at Tampere University of Technology, Department of Communications Engineering, Finland. He is the Editor-in-Chief of the *Computer Networks Journal* (Elsevier), and the founding Editor-in-Chief of the *Ad Hoc Networks Journal* (Elsevier), the *Physical Communication Journal* (Elsevier), and the *Nano Communication Networks Journal* (Elsevier). He is an IEEE Fellow (1996) and an ACM Fellow (1997). He has received numerous awards from IEEE and ACM. His current research interests are in nanonetworks, Long Term Evolution (LTE) advanced networks, cognitive radio networks, and wireless sensor networks.

Luigi Paura received the Dr. Eng. degree summa cum laude in Electronic Engineering in 1974 from the University of Napoli Federico II. From 1979 to 1984, he was with the Dept. of Biomedical, Electronic and Telecommunications Engineering, University of Naples Federico II, first as an Assistant Professor and then as an Associate Professor. Since 1994, he has been a Full Professor of Telecom.: first, with the Dept. of Mathematics, University of Lecce; then, with the Dept. of Information Engineering, Second University of Naples; and, finally, since 1998, he has been with the Dept. of Biomedical, Electronic and Telecom. Engineering, University of Naples Federico II. In 1985–86 and 1991, he was a visiting researcher at the Signal and Image Processing Lab, University of California, Davis. Currently, he is a full professor with the Dept. of Electric Engineering and Information Technology (DIETI), at the University of Naples Federico II. His research interests are mainly in digital communication systems and cognitive radio networks.